**Journal of Plankton Research** Vol.18 no.2 pp.163–184, 1996

# Diel vertical migration of zooplankton in the Northeast Atlantic

Karen J.Heywood

*School of Environmental Sciences, University of East Anglia, Norwich NR4 7TJ, UK*

**Abstract.** Acoustic Doppler current profiler (ADCP) data collected during August–September 1991 reveal the diel migration of zooplankton in the northeast Atlantic (50–60°N, 10–40°W). Volume scattering strength has been calculated, from which the speed and depth of migrations have been studied. There are usually at least two layers displaying nocturnal migration, one spending the day at depths of 300–400 m and the other at depths of 50–100 m. Reverse migrations are also found to be a common occurrence in the region studied. Usually, a surface layer begins to descend at dusk as soon as the upward migrating layer arrives in surface waters. Vertical velocity measured from the ADCP provides the first detailed direct measurements of the swimming speeds of the populations *in situ*, which are generally between 2 and 6 cm $s^{-1}$. Migrating animals within layers do not move in unison; the animals at the leading edge are moving back towards the centre of the layer.

## Introduction

Diel vertical migration (DVM) is observed for most species and orders of zooplankton, and has long been studied in the laboratory and *in situ* (see, for example, the review by Forward, 1988). The most common pattern is of ascent to the near-surface layers at dusk, and descent to a deeper layer at dawn, the intervening hours being spent at a relatively constant depth ('nocturnal migration'). A less common behaviour exhibits a slow descent following arrival at the surface at dusk, and a subsequent second ascent to the surface towards the end of the night, prior to the dawn descent ('twilight migration'). Other species or stages undergo 'reverse migration', whereby the zooplankton ascend at dawn and descend at dusk. In his review of zooplankton behaviour, Haney (1988) comments that although reverse migration is generally believed to be less common, there is little quantitative information on the frequency of each type of migration. Unless otherwise stated, DVM will here be assumed to refer to nocturnal migration.

DVM is generally believed to be the result of a compromise between the need to feed and the need to avoid predation (although other reasons have been suggested, such as the avoidance of damaging UV light; Haney, 1988). Under circumstances of limited food availability, there is evidence that migration does not take place (Wishner *et al.*, 1988). Light is believed to be the dominant controlling factor; its effects may include some or all of (i) initiating the ascent or descent, (ii) determining the speed of migration and (iii) constraining the maximum depth attained.

Enright (1977) observed larger upward migration speeds for copepods than had previously been seen (0.8–2.5 cm $s^{-1}$), but such values have been supported by more recent observations. For example, Wiebe *et al.* (1992) estimated swimming speeds of 1–6 cm $s^{-1}$ for copepods and euphausiids. Individual swimming speeds observed in the laboratory tend to be high (e.g. up to 10 cm $s^{-1}$ for *Euphausia pacifica*; Torres and Childress, 1983), whereas those for populations observed in the field are typically an order of magnitude smaller (e.g. 2 cm $s^{-1}$ for *Euphausia*

*krohni*; Angel, 1985). There are few direct measurements of vertical speeds in the field, and care is needed in deducing speeds from net samples at different times during the migration. Wiebe *et al.* (1992) noted that median depth individuals appeared to migrate faster than those at the leading edge. The euphausiids moved together, but the copepods moved more progressively with different portions of the population moving at different rates. Roe *et al.* (1984) observed that copepods did not migrate as compact populations; they also found that they arrived in near-surface waters at or after sunset. Speeds varied from 1 to 4 cm $s^{-1}$ both upward and downward.

As Haney (1988) comments, 'remote sensing with sonar is attractive for it is ideally suited for synoptic surveys and continuous monitoring of population movements... The greatest limitation is the difficulty in identifying the specific organisms responsible for the signals'. Acoustic techniques are non-invasive and can detect the larger zooplankton capable of swimming out of the way of nets. Prior to the 1980s, most acoustic studies of diel migration were conducted using single or multi-frequency fish detection echo sounders. More recently, the potential of the acoustic Doppler current profiler (ADCP), developed primarily for the precise determination of horizontal current velocity, has been recognized by those interested in zooplankton abundance and behaviour (Flagg and Smith, 1989; Plueddemann and Pinkel, 1989; Heywood *et al.*, 1991; Roe and Griffiths, 1993). Although it cannot offer the size determination of highly sophisticated multi-frequency acoustics (e.g. Wiebe *et al.*, 1990), it has become a standard tool of physical oceanographers and is widely available, and offers the exciting possibility of studying zooplankton in relation to their physical environment. In addition, it directly measures the vertical speed of the scatterers. The size of animals which will contribute most to the backscattered signal will depend on the frequency of sound used. Those much smaller than the sound wavelength will scatter little (Wiebe *et al.*, 1990). For a 153 kHz ADCP, the animals will be of order 1 cm.

Plueddemann and Pinkel (1989) showed that a Doppler sonar (similar to the ADCP) could detect diel migration. Vertical velocity anomalies from the mean velocity at each depth over a specified period were of the same order of magnitude as the vertical speed of the envelope of the peak in backscatter, but tended to be biased low due to a background of stationary scatterers. Three distinct scattering layers were observed, with daytime depths of ~300, 560 and 1000 m. Vertical migration rates varied between 1 and 4 cm $s^{-1}$, the deepest animals migrating the fastest. During the day, the scatterers remained at a constant depth and did not commence their ascent much before dusk. The observations spanned 13 days drifting on FLIP in the North Pacific off California; the patterns of diel migration were highly persistent during the period and over horizontal scales of ~50 km. Plueddemann and Pinkel's data set was obtained using a 67 kHz sonar with a maximum range of 1200 m. They calculate that the primary scatterers will have lengths of between 0.5 and 2.0 cm. They were only able to look at anomalies in backscatter and vertical speed at any particular depth since their sonar's output signal was not calibrated. Therefore, they would not have been able to distinguish a layer that was always higher or lower than those above or below, since the mean of each layer is subtracted.

Smith *et al.* (1989) used an uncalibrated 307 kHz ADCP (scattering primarily from animals of size 0.5 cm or larger) to study zooplankton patchiness, and estimated vertical migration rates of 5–8 cm $s^{-1}$ during ascent and of 3–4 cm $s^{-1}$ during descent from the peaks of backscatter. This difference between upward and downward speed suggested that this population may use gravity to sink rather than swim actively, as proposed by Rudjakov (1970). Most other studies find the migrations to be symmetrical (e.g. Plueddemann and Pinkel, 1989; Batchelder *et al.*, 1995). Fischer and Visbeck (1993) used moored ADCPs (153 kHz) to study DVM over a 1 year period in the Greenland Sea, highlighting the exciting possibilities of zooplankton studies under ice. Vertical velocity and relative backscattered energy were determined every 30 min. Strong seasonal variations were observed, maximum migration being observed in February–April and September–October. The daytime resting depth was shallower during the winter, with zooplankton migrating only 100 m compared to 350 m in the strongest migration periods. No migration was observed during May–July when daylight is nearly continuous. Vertical speeds were small (1–2 cm $s^{-1}$), with upward motion commencing immediately after sunset and downward migration finishing before dawn. Neither of these studies was able to determine absolute backscatter since output signal strength was unknown. More recently, there have been further quantitative comparisons between backscatter determinations from ADCP and abundance measurements from a comprehensive net survey [Zhou *et al.* (1994) in the Southern Ocean and Batchelder *et al.* (1995) in the North Atlantic]. Batchelder *et al.*'s (1995) study was in a similar area of the North Atlantic to that discussed in this paper, but took place ~3 months earlier during the spring bloom, and was a more localized survey.

In this paper, ADCP data collected during a cruise in the North Atlantic (Figure 1) are used to investigate the diel migration of scattering layers. The data cover an area some 2000 × 1000 km, where a variety of physical conditions were encountered, and show many examples of DVM at both dawn and dusk. All the data discussed were recorded off the continental shelf in regions of water depths of 1000–4000 m. Of particular interest are direct measurements of the migration velocities made by the ADCP and their relationship to the vertical layer movement.

## Data collection

In 1991 (1 August–4 September), an oceanographic survey (Figure 1) of the North Atlantic subpolar gyre was undertaken from RRS 'Charles Darwin' (Gould, 1992). Ninety-six full-depth CTD stations were completed, and continuous observations were taken using ADCP and a solar irradiance meter. Unfortunately, poor weather conditions were encountered during the cruise, which degraded the quality of the ADCP data—in particular, the noise was increased and the depth penetration decreased. The ADCP recorded backscattered signal strength from each of the four acoustic beams every 2 min. Vertical resolution was chosen to be 8 m; maximum range was ~400 m.

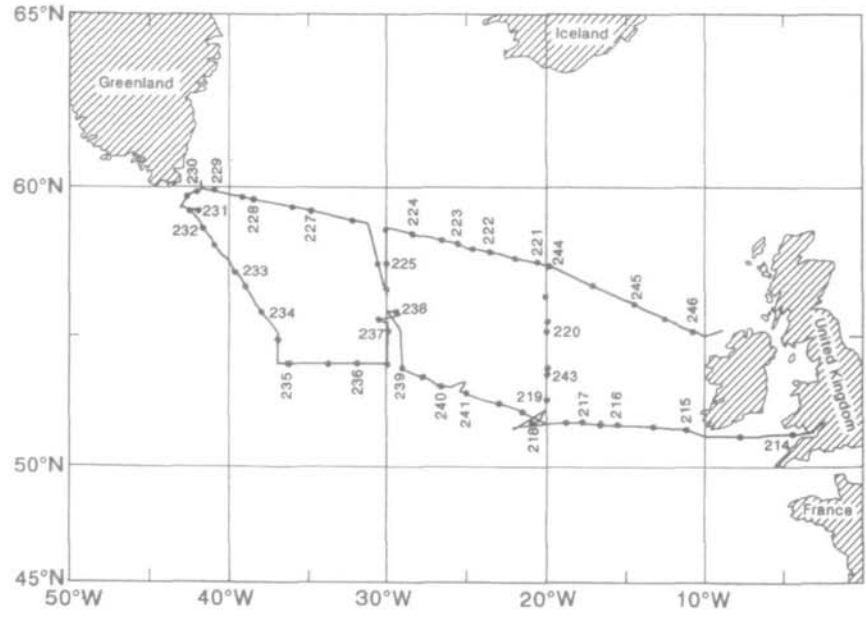


**Fig. 1.** Track plot of RRS 'Charles Darwin' cruise 62. The numbers along the track are the day of year and range from 214 (2 August 1991) to 246 (3 September 1991).

## Calculation of backscatter from ADCP

Early work on ADCP backscatter (Flagg and Smith, 1989; Heywood *et al.*, 1991) calculated only relative backscatter, since the manufacturers (RD Instruments, RDI) were then unable to provide an estimate of the strength of the sound signal output into the water. It is now possible for each ADCP to be calibrated by RDI and certain constants unique to each instrument determined. The signal output depends on the ship's supply voltage and upon a constant $K_1$ different for each of the four beams.

The following equation (RDI Technical Bulletin ADCP-90-04) was used to calculate the volume scattering strength, $Sv$ (Urick, 1983), for each of the four beams individually.

$$Sv = 10 \log_{10} \left\{ \frac{4.47 \times 10^{-20} K_2 K_s (T_x + 273)(10^{K_{cl}(E - E_r)/10} - 1) R^2)}{c_s P K_1 10^{-2\alpha R/10}} \right\}$$

where $R$ is the range to the bin, given by:

$$R = \left\{ \frac{B + \left| \frac{(P - D)}{2} \right| + ND + \frac{D}{4}}{\cos \theta} \right\} \frac{c_s}{1475.1}$$

$B$ is the blank distance adjacent to the transmitter, set by the user (4 m in this case). $P$ is the transmit pulse length, set by the user (8 m). $D$ is the length of each bin (8 m). $N$ is the number of the bin for which $Sv$ is to be calculated. $\theta$ is the angle of the

transducer beams to the vertical (30°). $c_s$ is the speed of sound, calculated from surface temperature and salinity for each profile. $K_2$ is the system noise factor measured by RDI during calibration, specific to each beam and each ADCP. $K_s$ is a constant depending on the frequency of the ADCP used. For a 153 kHz ADCP, it is $4.17 \times 10^5$. $T_x$ is the temperature (°C) of the transducer, recorded internally by the ADCP. $K_c$ converts from 'counts' into decibels. This parameter (dB per count) is a function of the temperature of the system electronics, $T_e$, which was logged throughout the cruise.

$$K_c = \frac{127.3}{(T_e + 273)}$$

$E$ is the parameter logged as AGC (acoustic gain control) by the ADCP DAS software, and is in fact echo intensity in 'counts'. The software records the intensity of the last ping in each 2 min ensemble. A different value of $E$ is obtained for each beam. $E_r$ is the noise value (counts) for that beam under the particular environmental conditions when the profile was obtained (see the discussion below).

$$K_1 = \left\{ \frac{(V_s a) - b}{c} \right\} K_{1c}$$

$a$, $b$ and $c$ are constants for the ADCP used; for a ship-mounted system with a nominal supply voltage of 220 V, values are 0.699, 4.27 and 37.14, respectively. $K_{1c}$ is a parameter measured by RDI during calibration, specific to each beam and each ADCP. $V_s$ is the supply voltage to the ADCP, checked regularly during the cruise (~240 V). $\alpha$ is the sound absorption coefficient (dB $m^{-1}$). It is a function of temperature, salinity and sound frequency (Urick, 1983). The determination of $\alpha$ is discussed below.

These equations were used to calculate $Sv$ during the entire cruise, except when the ship was in shallow water (<400 m). Arithmetic averages of the values for the four beams were calculated and will be the data discussed henceforth. Plots of $Sv$ for each of the four beams individually were found to show the same features, although they are more noisy. The diagrams of $Sv$ have been used to calculate the average speed of upward or downward layer motion during each migration, by tracking the maximum in backscattered signal intensity. Note that the ADCP cannot detect the presence of scatterers in the upper 10 m due to the depth at which it is mounted in the ship (5 m) and the depth blanked off (4 m).

### Sound absorption coefficient, α

The absorption of sound in the sea has been studied experimentally and empirical relationships derived considering the contributions due to pure water, boric acid and magnesium sulphate (Urick, 1983). The expressions used here are those due to Francois and Garrison (1982), who fitted a large global data set to expressions including depth, salinity, temperature, sound frequency and pH. A value of pH of

8.0 has been assumed and the ADCP frequency is 153 kHz. The remaining data were extracted from the CTD station data. The sound absorption coefficient was therefore allowed to vary spatially—significant variations are seen over the area of the North Atlantic discussed here (0.048–0.055 dB $m^{-1}$). In addition, $\alpha$ was calculated as a function of depth (typically varying from 0.05 near surface to 0.04 dB $m^{-1}$ at 400 m), and an average value calculated for the depth range through which the sound will have travelled to and from the scattering depth.

Figure 2 shows the effect of three different values of $\alpha$, 0.04, 0.05 and 0.06 dB $m^{-1}$, constant with depth. This particular example of an upward migration at dusk will be discussed later; it is shown in Figure 5 with $Sv$ calculated using the value of $\alpha$ deduced from *in situ* CTD measurements. Here we consider only the influence of varing $\alpha$. With the smallest sound absorption assumed (Figure 2a), backscattered intensities calculated further from the ADCP are decreased, while if a large sound absorption is assumed, the formula for $Sv$ predicts a greater density of scatterers at depth. Notice that in Figure 2a the ascending layer appears to intensify, while in Figure 2c the scattering layer thins as it rises; an artefact of the different sound absorption. The actual value of $\alpha$ used in Figure 5a is closest to Figure 2b, 0.05 dB $m^{-1}$, which clearly comes closest to conserving the total amount of backscattering in the water column and is likely to be the most realistic.

## Data quality control

Some care must be exercised in choosing ADCP data for analysis. Problems have previously been encountered in calculating backscatter using the ADCP on the RRS 'Charles Darwin' (Heywood *et al.*, 1991) since there is a large flow noise when the ship is steaming. Some other installations in other ships (e.g. Batchelder *et al.*, 1995) do not suffer this problem, in which case steaming data may be used with more confidence. Here the noise, $E_r$, is defined as the backscatter in the lowest bin (number 64), which is well after the point at which the ratio of signal plus noise to noise tends to one. Some calibrations were carried out in port and in the middle of the cruise in deep water, to determine the noise. This procedure is detailed in RDI Technical Bulletin ADCP-90-04. It was found that the noise level for each of the four beams was substantially different, as expected, and that the noise level when the ship was on station was constant throughout the cruise. This value agreed with the value obtained in port and during the calibration procedures. A 'noise floor' was chosen for each beam (13, 13, 23 and 29 counts for beams 1–4, respectively). When processing the data, any profile was rejected where the noise was more than 10 counts greater than this floor. In addition, backscatter was set to absent in any particular bin if the signal strength was <5 counts greater than the noise, $E_r$, or if the percentage of good pings was <5%. This eliminates data points where the signal to noise ratio is very low. Since data were only considered when the noise value was low, and this occurred when the ship was on station or steaming slowly, only 13 of the possible 63 dawns or dusks during the cruise (2 August–3 September) were studied. Of these, seven have been chosen to represent the typical range of characteristics of scattering layers encountered during the cruise. All the data shown here are from periods when the ship was maintaining position over the CTD for a good wire angle.

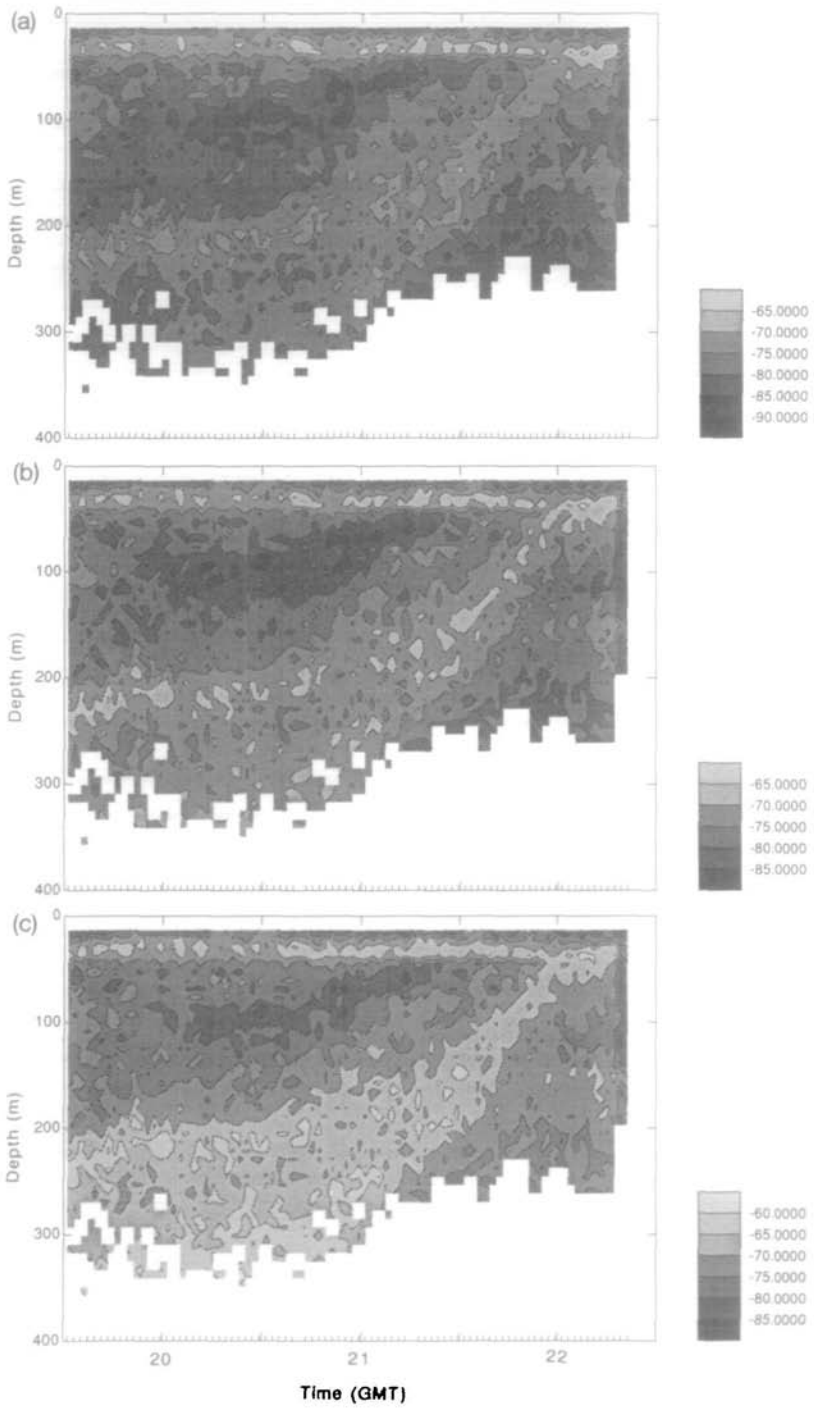


**Fig. 2.** Comparison of values of *Sv*, the backscattered signal strength (dB), calculated from the ADCP, using values of the sound absorption coefficient $\alpha$ of (**a**) 0.04 dB $m^{-1}$, (**b**) 0.05 dB $m^{-1}$ and (**c**) 0.06 dB $m^{-1}$, respectively.

## ADCP vertical velocity and numerical simulation

Although principally intended to measure the horizontal components of velocity, the ADCP also calculates and records the vertical component. It measures the speed of the scatterers rather than the water itself. Usually the scatterers are assumed to be advected passively with the water. In the case of horizontal velocities, the swimming speed of the plankton is negligible in comparison to the water movement [except under exceptional circumstances; see, for example, Wilson and Firing (1992)]. For vertical velocities, the water upwelling or downwelling is usually small under general oceanic conditions, except during events such as internal waves. This paper considers vertical velocity during the periods of diel migration, and claims that the vertical swimming of the zooplankton is directly measured by the ADCP.

When the ship is steaming, values of vertical velocity are very erratic and not to be believed. Therefore, the same screening has been applied to the vertical velocity as was applied to the backscatter data. Other authors (e.g. Roe and Griffiths, 1993) determine the vertical velocity anomaly at each depth by subtracting the mean over a long period or distance, but this approach has not been found necessary here (probably because periods of fast steaming are excluded by the stringent noise criterion).

To test the validity of the vertical speeds observed by the ADCP, a numerical simulation was undertaken. This models the distribution of scatterers as a function of depth and time. The scatterers are moved vertically between bins in the model according to the vertical speeds measured by the ADCP, assumed to represent the swimming of the animals. Figure 3 illustrates the scenario envisaged and defines the variables of the model. Bin number $n$ has a vertical thickness of $\Delta Z$ (here 8 m) and an initial amount of scatterers zoo($n$). After time $\Delta t$ (here 120 s), the new amount of scatterers zoo′ ($n$) is calculated using the following equation:

$$\text{zoo}'(n) = \text{zoo}(n) - \frac{w(n).\Delta t.\text{zoo}(n)}{\Delta Z} + \frac{w(n+1).\Delta t.\text{zoo}(n+1)}{\Delta Z}$$

The observed ADCP vertical velocities $w(n)$ and $w(n+1)$ are strictly in the centre of the bin, but the error involved in assuming it to be valid at the boundaries between bins is negligible. If one or both of the vertical velocities is downward, then the equation is adapted to transport scatterers out of the upper bin into the lower one.

The model was initialized using the observed volume scattering strength $Sv$ at the beginning of the simulated time period in each 8 m vertical bin from the near surface to 400 m. There is no spin-up time before the model runs shown in subsequent diagrams. The procedure was to run the model forward in time, producing a new depth distribution every 2 min, for comparison with the observed scatterers. Note that, since $Sv$ is logarithmic, it was necessary to take antilogs before adding or subtracting animals from each 8 m bin, and then convert back to decibels at the end of the time step. Total numbers were conserved by allowing no vertical flux at the surface or at 400 m.

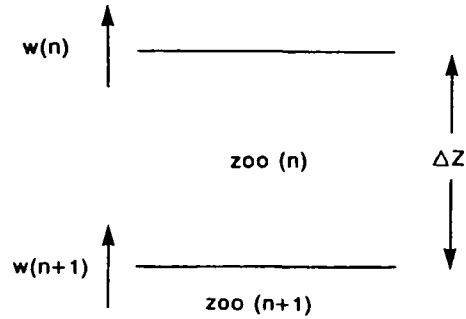


**Fig. 3.** Schematic diagram of the numerical simulation procedure and variables.

To allow a simple quantitative comparison between the simulated and observed values of $Sv$, the root-mean-square (rms) difference between the two values was calculated for each simulated period, normalized by the observed value of $Sv$. This quantity, designated $Q$, is calculated using the following equation, where $k$ is the number of bins in depth and time where valid values of the observed and simulated scattering field are available.

$$Q = \log \frac{\sqrt{\sum_{1}^{k} \left( \frac{\exp(Sv(\text{simulated})) - \exp(Sv(\text{observed}))}{\exp(Sv(\text{observed}))} \right)^2}}{k}$$

Again this had to be calculated on the non-logarithmic values, hence the calculation of the antilogs. A larger value for this indicates that the simulated backscattering field is substantially different from that observed, whereas a smaller value indicates that the simulation is reasonable. For the examples shown here, values for $Q$ range from $1.0 \times 10^{-3}$ dB for a good simulation to $1.9 \times 10^{-3}$ dB for a poor simulation.

## Results

*Day 216 (4 August; 52°N, 17°W)*

The dusk migration of three separate scattering layers can be seen in the contoured backscattered signal intensity (Figure 4a). All times displayed on figures are GMT, not local time. Lighter shades denote larger backscattered intensities, thus greater densities of zooplankton. The shallowest layer has spent the daylight hours near 100 m and rises slowly (with an average speed of 0.8 cm $s^{-1}$) to arrive in the upper 50 m at 21:00. It follows fairly closely the 0.2 W $m^{-2}$ isolume, calculated from the surface solar radiation assuming a simple two-exponential decay in class II waters. Two deeper layers are revealed: one apparently rising from ~250 m and one moving rapidly from a deeper depth; these arrive near the surface at about 21:30 and form a large area of plankton in the upper 50 m during the night. The deeper layers do not follow isolumes. The rapid upward migration starts at about 20:30, which coincides with the onset of total darkness. In the vertical speed diagram (Figure 4b), lighter shades denote upward motion and dark shades downward motion. The

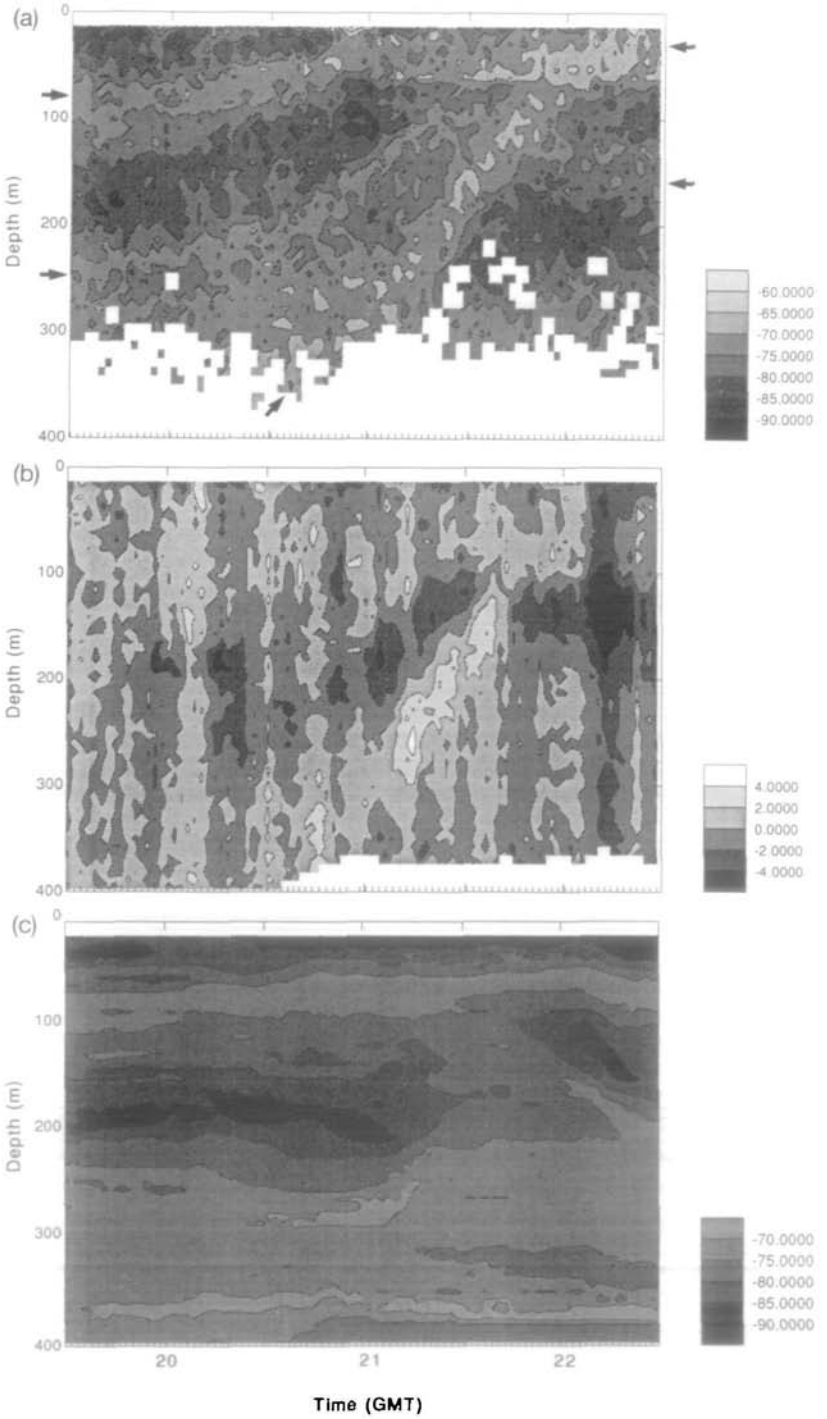

speeds indicated for the deepest layer, which peak at 4 cm $s^{-1}$, are somewhat smaller than that determined from the signal intensity (Figure 4a), 6 cm $s^{-1}$.

The simulation (Figure 4c) shows a layer (again denoted by lighter shades, indicating larger numbers of animals) beginning to migrate upwards from ~300 m at 21:00, as measured by the backscatter (Figure 4a), but it cannot distinguish the two deeper layers. The rapid rise at about 21:30 is not adequately reproduced, presumably because the ADCP vertical velocities are too small. The simulation parameter $Q$ for this period is $1.3 \times 10^{-3}$ dB. The ADCP vertical speeds are likely to be biased low by non-migratory scatterers in the ensonified volume. The near-surface scattering layer (50–100 m) is also revealed by the model, and indeed the vertical velocities suggest that it may be this layer which is descending to 200 m (reverse migration) at the same time as the larger layer is migrating upwards.

*Day 218 (6 August; 52°N, 20°W)*

At dusk on day 218 (Figure 5a), a distinct layer is seen migrating towards the surface containing some scatterers from 230 m and another population from deeper than 300 m. The vertical speed (Figure 5b) shows that the upper part of the scattering layer is moving downwards, while the lower part moves upwards. Upward speeds are greater than downward, as one would expect since the layer as a whole migrates upwards. Notice also that the layer thins and becomes more concentrated as it rises. A thin surface layer remains at ~30 m throughout; the particles in the low scattering region below this are moving upwards to join this layer.

The vertical velocities are too small for the model to adequately predict the complete ascent at dusk (Figure 6c). However the beginning of the ascent is simulated and the difference $Q$ between Figure 5a and c was calculated at $1.5 \times 10^{-3}$ dB. The vertical velocities (Figure 6b) show a large downward motion at about 22:00, again suggesting reverse migration co-existing, and this prevents the model from completing the upward motion of the main scattering layer.

*Day 220 (8 August; 56°N, 20°W)*

Day 220 shows the clearest and most compact layer migrating downwards at dawn (Figure 6). Its thickness is 30–40 m. It also has the highest backscatter of any layer observed; in places over −60 dB compared to background values of less than −80 dB. The layer migrates from night-time levels of ~30 m to below 300 m; later that day, there was an indication of a layer at 350 m. There was no significant shallower layer during the day here. The vertical speed (Figure 6b) does not show a distinct region of downward migration, rather a diffuse area with peak downward speeds of 2–3 cm $s^{-1}$. The peak of the backscatter also shows a downward speed of that magnitude: 2.7 cm $s^{-1}$. The migration is simulated reasonably (Figure 6c), with a value of $Q$ of $1.4 \times 10^{-3}$ dB. The migration starts at least 1 hour before there is any increase in solar radiation detected by the solarimeter. It is considerably faster than could be accommodated by following isolumes.

**Fig. 4.** Diel migration at dusk, day 216. Times marked are in GMT. (**a**) *Sv*, the backscattered signal strength (dB), calculated from the ADCP. Blank areas indicate where the data do not satisfy the quality criteria discussed in the text. Scattering layers are marked by arrows. (**b**) Vertical velocity measured by ADCP. (**c**) Numerical simulations of vertical migration using observed vertical velocities. The model was initialized at the beginning of the period shown (in this case, 19:30).

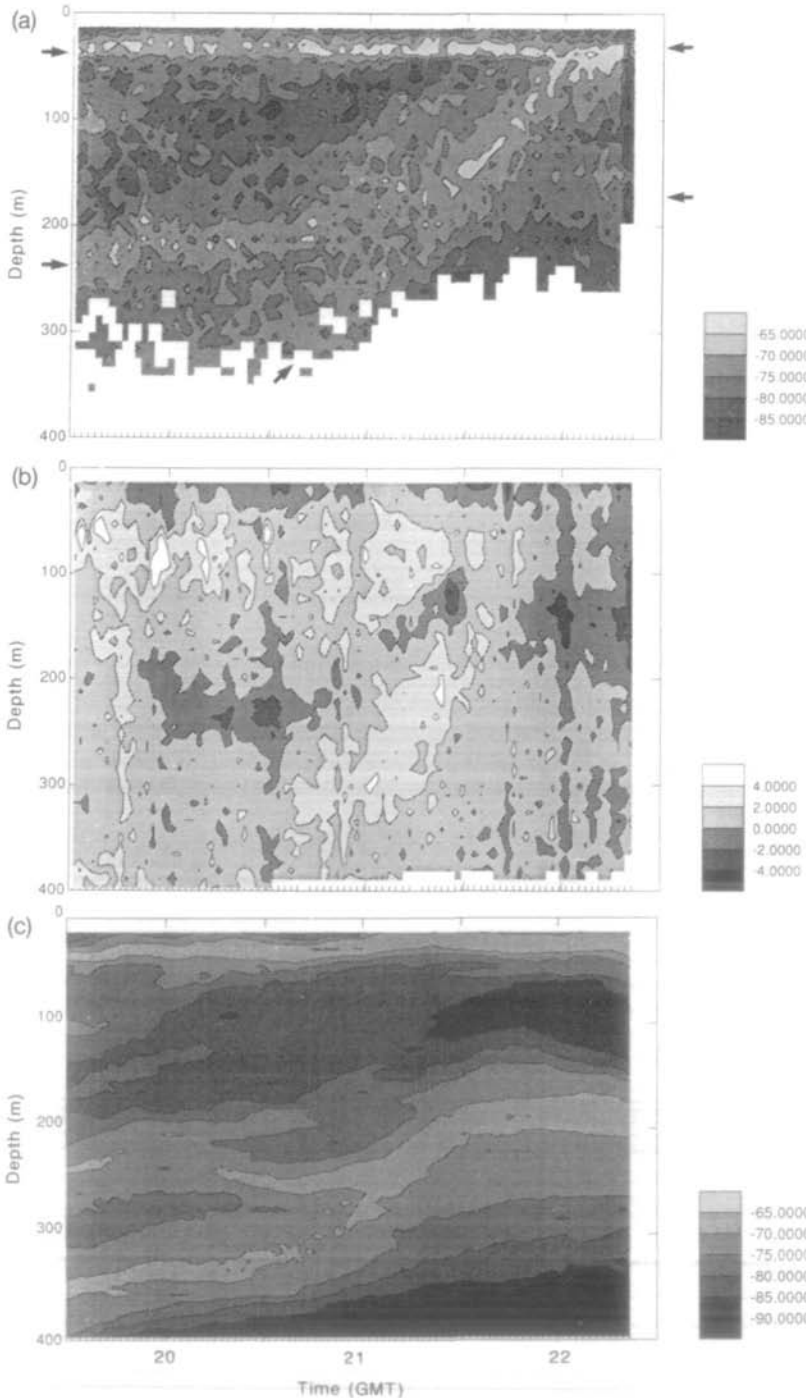


**Fig. 5.** Diel migration at dusk, day 218. Otherwise as Figure 4.

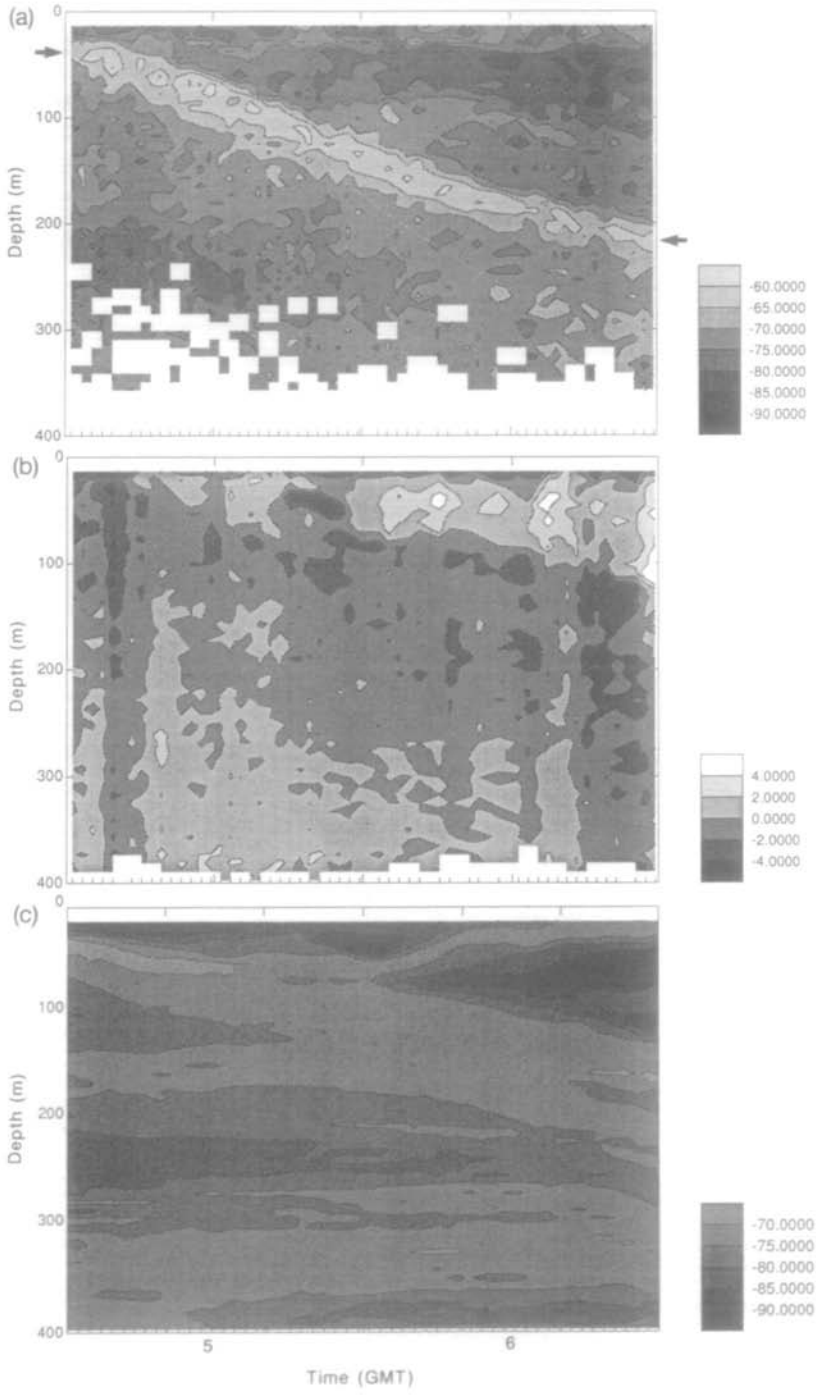


**Fig. 6.** Diel migration at dusk, day 220. Otherwise as Figure 4.

*Day 239 (27 August; 53°N, 27°W)*

Figure 7, showing dawn on day 239, displays a diffuse downward movement of the main scattering layer, which gets noticeably more dense as it descends. The vertical speeds show a distinct boundary between upward and downward moving scatterers. The maximum speed, up to 4 cm $s^{-1}$, coincides with the maximum backscatter. The scattering layer indicates a vertical migration rate of 3 cm $s^{-1}$, very much in agreement with the speed directly measured. The migration commenced at least 1 h before first light was detected by the solarimeter. Notice also the thin (~10 m thick) scattering layer at ~50 m during daylight.

The migration is well simulated (Figure 7c), for both the scattering layer moving down to 300 m, and the thin layer at 50 m depth. The rms difference $Q$ is calculated to be $1.3 \times 10^{-3}$ dB.

*Day 240 (28 August; 53°N, 25°W)*

Reverse migration is seen clearly on day 240 (Figure 8). The most pronounced layer rises at dusk from deeper than 300 m to form a night-time layer at ~40 m. Simultaneously a second, thinner layer, which has spent the day at ~40 m, descends to around 200 m. Because the two layers cannot be clearly distinguished as they cross, migration speeds estimated from the movement of the peak scattering may be erroneous. Figure 8b shows that the scatterers near the surface at 21:30 are part of the downward migration rather than the upward one. Both the ascending and descending layers have speeds of the order of 4 cm $s^{-1}$. The vertical speed (Figure 8b) shows both the upward and downward migrations. The upward moving layer has vertical speeds of 2–4 cm $s^{-1}$, while the downward moving layer shows speeds in excess of 4 cm $s^{-1}$. The reverse migration appears to be triggered either by the arrival of the other scattering layer, or by sunset. These data were collected very close to the Polar Front associated with the North Atlantic Current.

The model can barely cope with such a complex situation (Figure 8c), where one layer is undergoing nocturnal migration and another layer of similar size is showing reverse migration. Such a structure would probably not be revealed by a net study, and interpretation of the scattering data without the vertical velocity data would be open to question. The model emphasizes the reverse migration, since the vertical speeds are larger, and accurately predicts the rate and depth of descent. The difference parameter $Q$ is found to be $1.7 \times 10^{-3}$ dB, a relatively large value despite the apparent agreement 'by eye'. This is probably due to the scatterer-free region which develops in the model; possibly in the real data scatterers are entering the modelled zone from above the depths measured by the ADCP.

*Day 241 (29 August; 53°N, 23°W)*

Day 241 shows dusk migrations (Figure 9) between ~30 and 350 m which again are unrelated to isolume depths. A reverse migration is indicated just after dusk, which falls at 20:20. The upward migration is interesting since two layers are involved. A shallower one moves upwards more gradually from ~300 m, while a thinner layer is moving upwards from some deeper level more rapidly. The vertical speed plot (Figure 9b) shows the movement of these two layers, the upper one showing

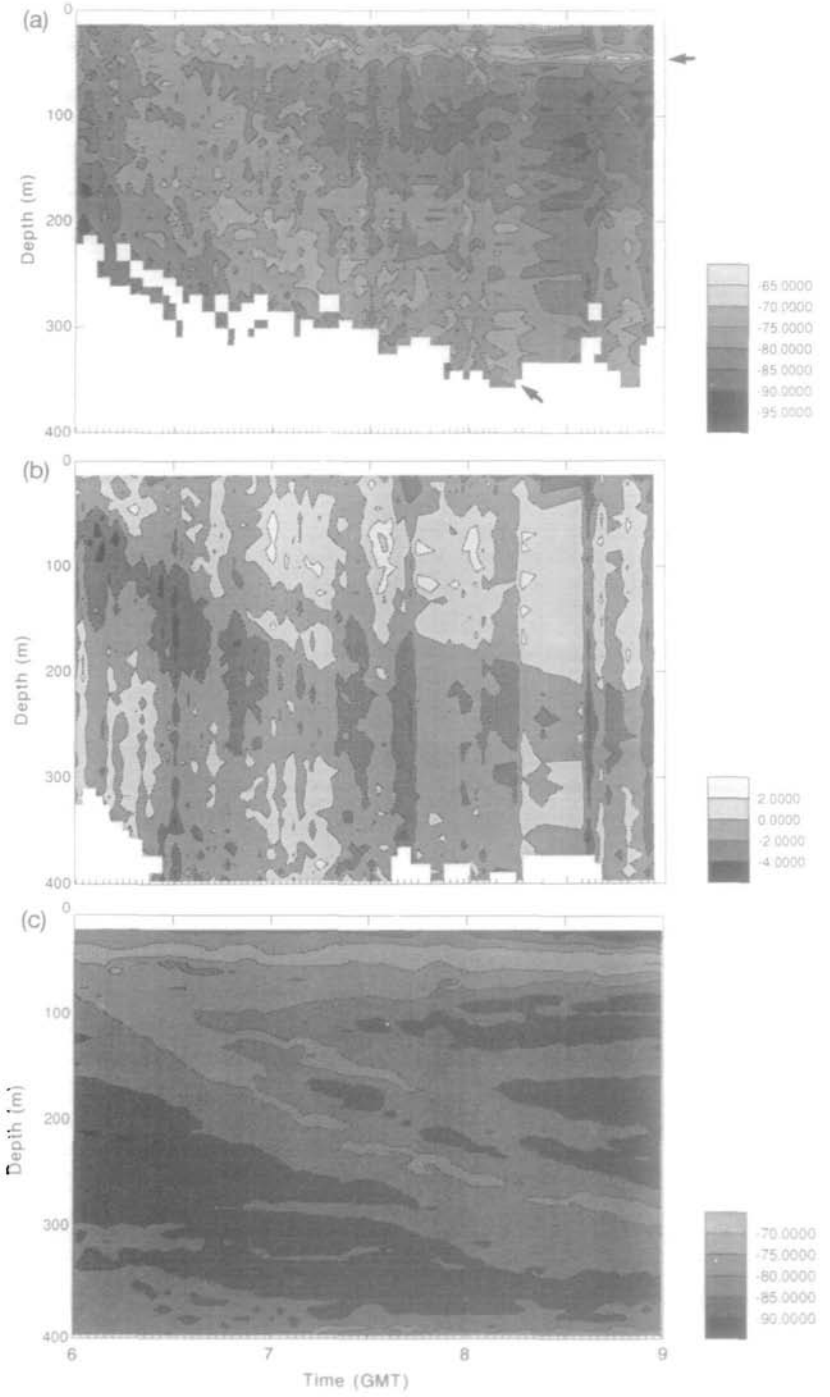


**Fig. 7.** Diel migration at dusk, day 239. Otherwise as Figure 4.

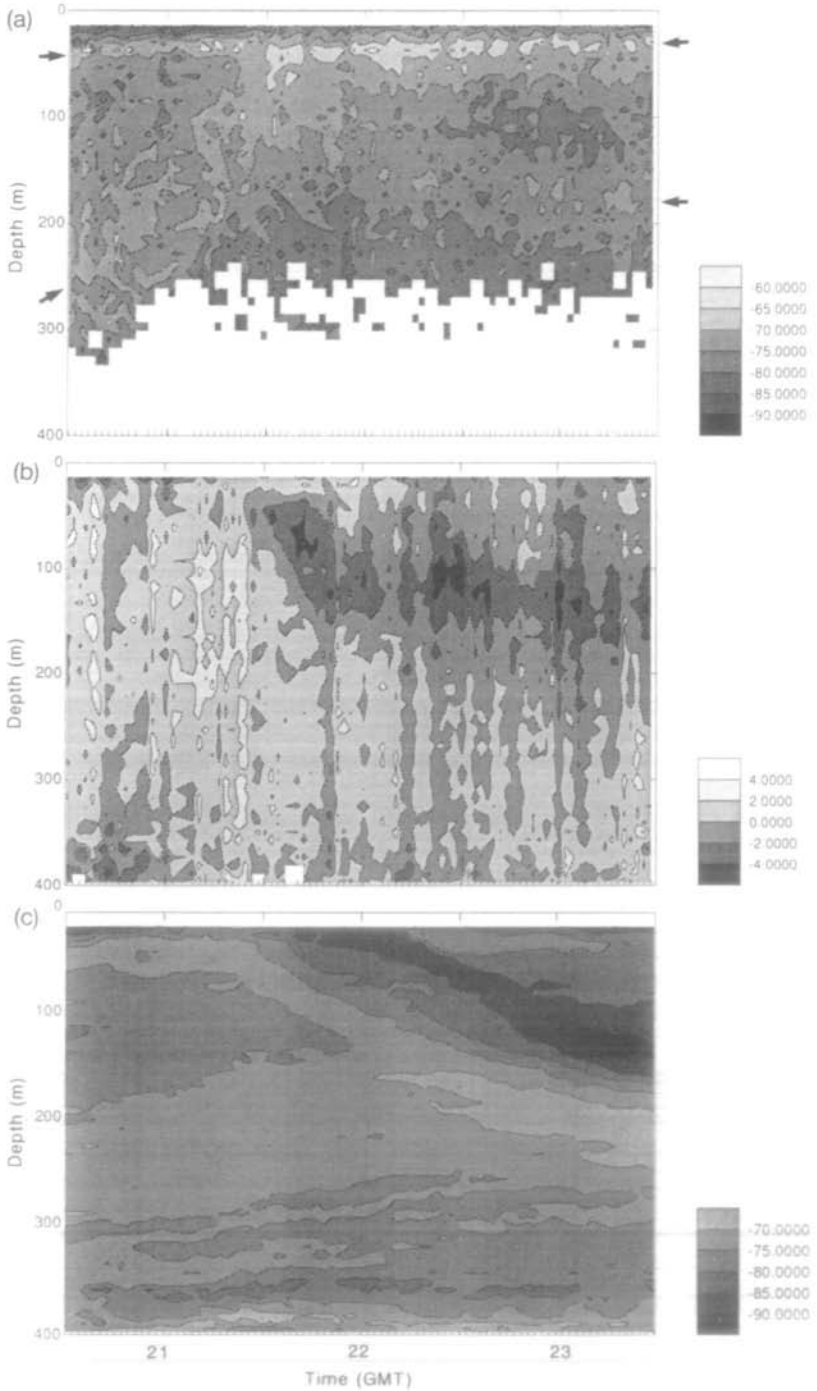


**Fig. 8.** Diel migration at dusk, day 240. Otherwise as Figure 4.

speeds of ~2 cm $s^{-1}$, the lower one between 2 and 4 cm $s^{-1}$. The distribution of scatterers during the night appears to be more diffuse than usual, with a broad layer remaining between 150 and 200 m. Again the reverse migration seems to be triggered either by the arrival of competitors (or predators) or by sunset. The simulated distribution (Figure 9c) reveals this complexity and some of the features observed in the scattering data are reproduced: the main layer leaving 300 m to migrate upwards, a further layer appearing at a greater depth and the reverse migration commencing at 20:30. The simulation is a poor one, showing the largest value of $Q$, $1.9 \times 10^{-3}$ dB.

*Day 246 (3 September; 55°N, 10°W)*

The final diel migration was seen at dawn on day 246 (Figure 10). Two distinct layers are apparent, both of which start their downward movement at about 05:00, about an hour before any measurable increase in solar radiation. A broad, deeper layer migrates from ~40 to 350 m, fairly rapidly (the speed is not well defined since the peak is diffuse, but is between 6 and 9 cm $s^{-1}$). The vertical speed recorded is 2–4 cm $s^{-1}$. A thin, well-defined upper layer migrates more slowly from a similar depth to ~120 m (speed around 1 cm $s^{-1}$, while the vertical speed is between 0 and 2 cm $s^{-1}$). The simulation (Figure 10c) exhibits a well-simulated main layer descending to ~350 m, but the slower downward migration of the near-surface layer is not well predicted. For both layers, the rate of descent is too small. This simulation gives the smallest rms difference between observations and model, $Q = 1.0 \times 10^{-3}$ dB.

## Discussion

It is not possible to identify the zooplankton orders or species whose migration has been discussed (there are clearly several). Since they will be of order 1 cm in size, they are likely to be copepods, euphausiids and amphipods. Roe and Griffiths (1993) suggest that the most likely contributors to ADCP backscatter in the north-east Atlantic would be the euphausiid *Meganyctiphanes norvegica* and the amphipod *Themisto compressa*. Fischer and Visbeck (1993) suggest that their 153 kHz ADCP in the Greenland Sea is observing the euphausiid *Thyssanoessa longicaudata*, but the vertical speeds they observed (of order 1 cm $s^{-1}$) are generally smaller than those discussed here. Investigations in the Kattegat (quoted by Fischer and Visbeck) also suggested *M.norvegica* as a likely candidate for fast migrations observed by ADCP. A further possibility is that some layers may be small fish, such as the dominant myctophid *Benthosema glaciale* (M.Angel, personal communication). Batchelder *et al.*'s (1995) comprehensive net survey in very much the same area as discussed here, but 3 months earlier, suggests that *Calanus finmarchicus* may be the likely scatterer in this region.

It should be noted that where ADCP data were good enough, diel migrations were always seen throughout the cruise. They are therefore persistent in both time and space. All the examples discussed here show nocturnal migration. In addition, reverse migration is revealed to occur in half of the cases discussed—the same proportion was apparent in days not shown here. It would appear that, at least at dusk, a layer mirrors the nocturnal migration: as soon as the deep layer reaches the

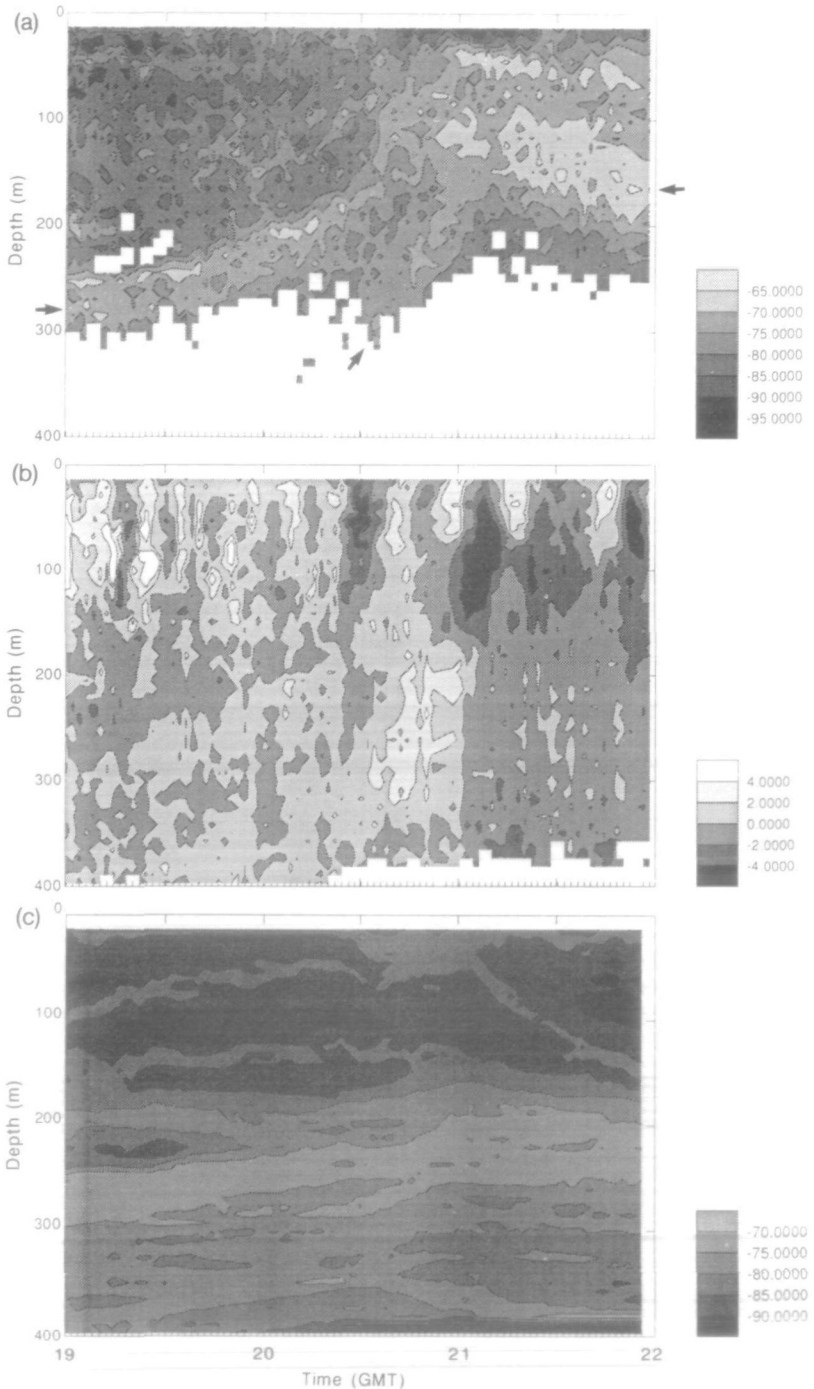


**Fig. 9.** Diel migration at dusk, day 241. Otherwise as Figure 4.

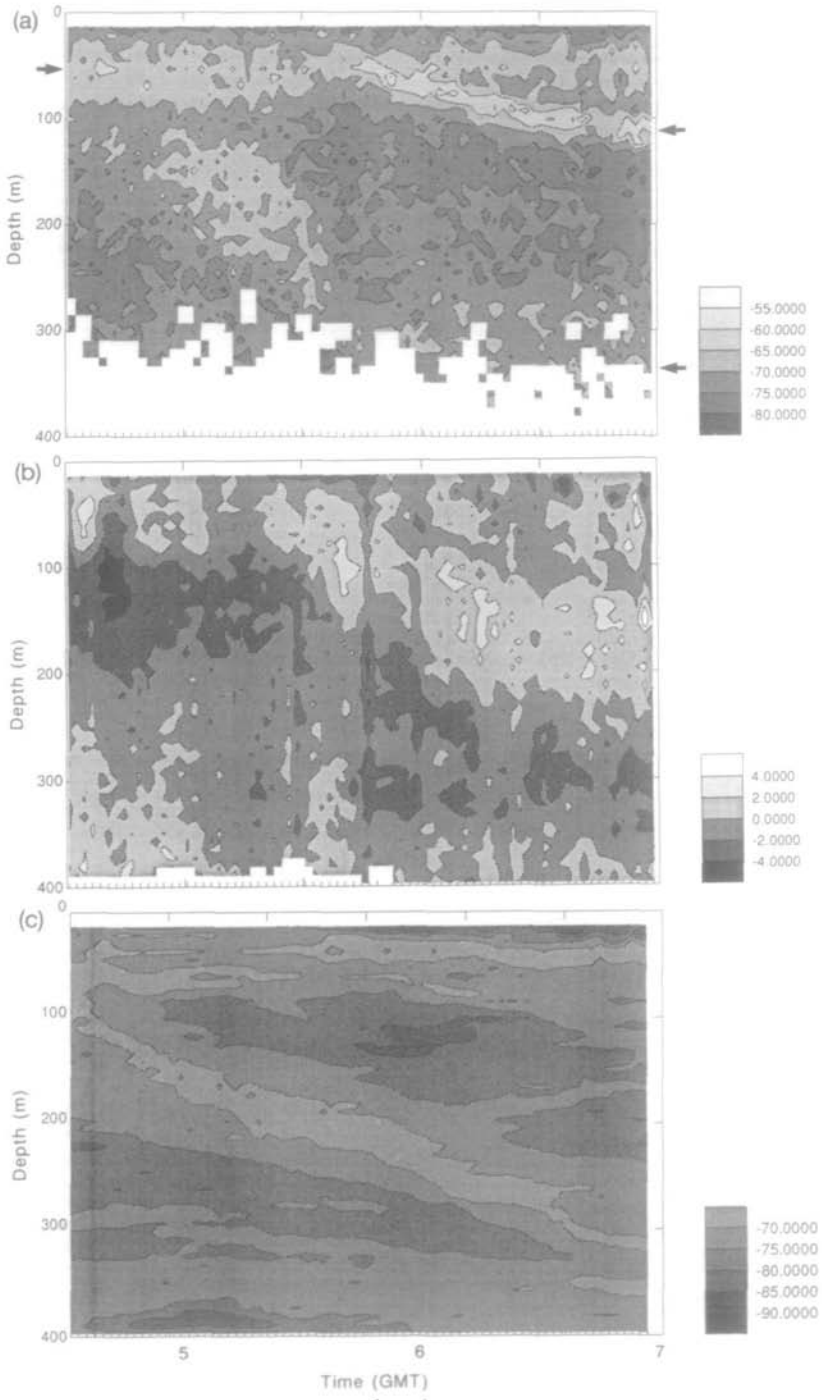


**Fig. 10.** Diel migration at dusk, day 246. Otherwise as Figure 4.

surface, another near-surface layer starts a downward migration. This reverse migration is not coincident with the onset of total darkness or with a maximum in the rate of change of solar radiation. Rather, it seems to be correlated with the arrival of the other layer, which may be predators or competitors. Such detailed observations of behaviour are possible only using acoustic methods such as the ADCP; furthermore, the vertical velocity information which the ADCP provides is valuable in identifying whether plankton within layers are in fact moving upwards or downwards. The observations at dawn neither support nor rule out the ubiquity of reverse migration in this region, since the periods of good data do not start sufficiently before dawn.

The Polar Front, marking the core of the North Atlantic Current, turns north at ~52°N, 20°W, but it is believed that a lesser branch continues to the east to 15°W where it meets waters from the south and turns north. The observations shown here span both sides of the Polar Front, from warmer, saltier waters to the south-east to cooler, fresher waters to the north and west. Mixed layer depths varied from 10–20 m to the east of the Polar Front to 50–60 m to the west of it. Scattering layers observed throughout the cruise had a tendency during their near-surface period to be located in the pycnocline, at the peak(s) in stratification just below the mixed layer. They were usually associated with a decrease in dissolved oxygen concentration.

ADCP speeds are consistently smaller than those of peak in scattering. Plueddemann and Pinkel (1989) also found the Doppler velocities to be biased low, and explained that this will be due to a background of non-migrating scatterers. They believed the migrators to be a small proportion of the scattering field; as this proportion increases, the Doppler velocities will more fairly represent the speed of the migrating animals. Nevertheless, one should be aware that the scattering layer itself can move faster than any of its constituent individuals. The simple simulation of the scattering layers by applying the observed ADCP vertical velocities has demonstrated that the Doppler currents are able to provide the necessary migration speeds. The downward migrations are generally simulated better than upward ones, suggesting that there may be a small bias in the vertical speeds measured by the ADCP.

The layers which migrate only within the upper 100 m do appear to migrate following isolumes and their motion may be initiated by changes in the relative rate of change of solar radiation. However, most scattering layers migrate to ~400 m, and these ascend and descend more rapidly than the isolumes. They consistently pre-empt dawn by ~1 h. It is known that some species may have an internal clock which is reset daily. Might it also be possible that some species can detect light at the UV end of the spectrum, where dawn would appear more than half an hour before it would be evident in the visible? Forward (1988) discusses the sensitivity of zooplankton to spectral differences, and most evidence suggests a peak sensitivity in the blue–green which penetrates most deeply in ocean waters. No determination of their sensitivity to UV is mentioned. Animals who could react more promptly to dawn by detecting UV light before dawn is apparent in the visible band would have an advantage over their competitors. Although some freshwater fish have been shown to have UV vision, Partridge (1990) concludes that 'the

importance of ultra-violet vision in marine fish is speculative'. Adult fish tend not to have lenses that are transparent to UV light, whereas juveniles or larvae do, so he suggests that by analogy with freshwater fish, sensitivity to UV light is most likely to be found in larvae or juveniles living in areas of low levels of *Gelbstoff*, such as the open ocean of the northeast Atlantic.

The ADCP vertical currents show that the zooplankton like to keep together: during upward migrations, the upper animals move down towards the centre of the layer and during downward migrations the lower animals move upwards into the layer. The numerical simulation supported the validity of these observations in the vertical velocities. Wiebe *et al.* (1992) also observed that the 'median depth individuals as a whole appeared to migrate faster than their leading edge counterparts'.

## Acknowledgements

I wish to thank Dr John Gould, Principal Scientist of RRS 'Charles Darwin' cruise 62. This work was supported by NERC grant GR9/581 and my participation in the cruise by NERC WOCE Special Topic grant GST/02/576. I am grateful to Dr Martin Angel (IOSDL) for valuable suggestions and to an anonymous referee for helpful and constructive criticism.

## References

Angel,M.V. (1985) Vertical migrations in the oceanic realm: Possible causes and probable effects. In Rankin,M.A. (ed.), *Migration: Mechanisms and Adaptive Significance. Port Aransas: Mar. Sci. Inst., Contrib. Mar. Sci.*, **27(Suppl.)**, 45–70.

Batchelder,H.P., VanKeuren,J.R., Vaillancourt,R. and Swift,E. (1995) Spatial and temporal distributions of acoustically estimated zooplankton biomass near the Marine Light-Mixed Layers station (59°30′N, 21°00′W) in the North Atlantic in May 1991. *J. Geophys. Res.*, **100**, 6549–6563.

Enright,J.T. (1977) Copepods in a hurry: sustained high-speed upward migration. *Limnol. Oceanogr.*, **22**, 118–125.

Fischer,J. and Visbeck,M. (1993) Seasonal variation of the daily zooplankton migration in the Greenland Sea. *Deep-Sea Res.*, **40**, 1547–1557.

Flagg,C.N. and Smith,S.L. (1989) On the use of the acoustic Doppler current profiler to measure zooplankton abundance. *Deep-Sea Res.*, **36**, 455–474.

Forward,R.B. (1988) Diel vertical migration: zooplankton photobiology and behaviour. *Oceanogr. Mar. Biol. Annu. Rev.*, **26**, 361–393.

Francois,R.E. and Garrison,G.R. (1982) Sound absorption based on ocean measurements. *J. Acoust. Soc. Am.*, **72**, 1879–1890.

Gould,W.J. (1992) *RRS Charles Darwin* Cruise 62, 01 Aug–04 Sep 1991, CONVEX-WOCE Control Volume AR12. *IOSDL Cruise Report No. 230*, 60 pp.

Haney,J.F. (1988) Diel patterns of zooplankton behaviour. *Bull. Mar. Sci.*, **43**, 583–603.

Heywood,K.J., Scrope-Howe,S. and Barton,E.D. (1991) Estimation of zooplankton abundance from shipborne ADCP backscatter. *Deep-Sea Res.*, **38**, 677–691.

Partridge,J.C. (1990) The colour sensitivity and vision of fishes. In Herring,P.J., Campbell,A.K., Whitfield,M.R. and Maddock,L. (eds), *Light and Life in the Sea*. Cambridge University Press, pp. 167–184.

Plueddemann,A.J. and Pinkel,R. (1989) Characterization of the patterns of diel migration using a Doppler sonar. *Deep-Sea Res.*, **36**, 509–530.

Roe,H.S.J. and Griffiths,G. (1993) Biological information from an acoustic Doppler current profiler. *Mar. Biol.*, **115**, 339–346.

Roe,H.S.J., Angel,M.V., Badcock,J., Domanski,P., James,P.T., Pugh,P.R. and Thurston,M.H. (1984) The diel migrations and distributions within a mesopelagic community in the North East Atlantic. *Prog. Oceanogr.*, **13**, 245–511.

Rudjakov,J.A. (1970) The possible causes of diel vertical migrations of planktonic animals. *Mar. Biol.*, **6**, 98–105.

Smith,P.E., Ohman,M.D. and Eber,L.E. (1989) Analysis of the patterns of distribution of zooplankton aggregations from an acoustic Doppler current profiler. *CalCOFI Rep.*, **30**, 88–103.

Torres,J.J. and Childress,J.J. (1983) Relationship of oxygen consumption to swimming speed in *Euphausia pacifica*. 1. Effects of temperature and pressure. *Mar. Biol.*, **74**, 79–86.

Urick,R.J. (1983) *Principles of Underwater Sound*. McGraw-Hill, New York, 423 pp.

Wiebe,P.H., Greene,C.H., Stanton,T.K. and Burczynski,J. (1990) Sound scattering by live zooplankton and micronekton: empirical studies with a dual-beam acoustical system. *J. Acoust. Soc. Am.*, **88**, 2346–2360.

Wiebe,P.H., Copley,N.J. and Boyd,S.H. (1992) Coarse-scale horizontal patchiness and vertical migration of zooplankton in Gulf Stream warm-core ring 82-H. *Deep-Sea Res.*, **39(Suppl.)**, S247–S278.

Wilson,C.D. and Firing,E. (1992) Sunrise swimmers bias acoustic Doppler current profiles. *Deep-Sea Res.*, **39**, 885–892.

Wishner,K., Durbin,E., Durbin,A., Macaulay,M., Winn,H. and Kenney,R. (1988) Copepod patches and right whales in the Great South Channel off New England. *Bull. Mar. Sci.*, **43**, 825–844.

Zhou,M., Nordhausen,W. and Huntley,M. (1994) ADCP measurements of the distribution and abundance of euphausiids near the Antarctic Peninsula in winter. *Deep-Sea Res.*, **41**, 1425–1445.

*Received on November 25, 1994; accepted on October 13, 1995*